 CMES, vol.41, no.2, pp.95-106, 2009

An Atomistic Study of Elliptic Cross-Sectional Nanosprings

I-L. Chang[1] **and M.-S. Yeh**[1]

Abstract: One-dimensional copper nanospring with elliptic cross section was studied using molecular statics method based on minimum energy consideration. Various geometric sizes (wire semi-axis length, radius, pitch) and crystal orientations of nanosprings were systematically modeled to investigate the size dependence of elastic properties for both normal and binormal nanosprings. It was observed that as the wire semi-axis increases, and the radius and pitch decrease, the nanospring stiffness would increase irrespective to the crystal orientations. Moreover, it was noticed that the normal nanosprings always behave stiffer than the binormal ones for the same radius, pitch and cross-sectional geometry in our study.

Keywords: Nanospring, molecular statics, spring constant, elliptic cross-section.

1 Introduction

Considerable research effort has been focused recently on one-dimensional nanostructures such as nanorods, nanowires, nanotubes and their assembled structures due to the possible applications and new physical phenomena. Among them, helical nanowires and coiled nanotubes (referred hereafter generally as nanosprings) are a new form of one-dimensional nanostructures that have promising applications in nanoelectromechanical systems [Singh, Liu, Ye, Picu, Lu, and Wang (2004), Gao, Ding, Mai, Hughes, Lao, and Wang (2005), Wang (2004)]. Nanosprings could be employed to measure an extremely small force of several nanonewtons and provided as an excellent energy dissipation mechanism. With the recent advance in nanotechnology, there is a growing interest in studying how the mechanical properties of the nanostructured materials differ from those of their bulk counterparts.

Various fabrication methods commonly used in semiconductor industry have been proposed to synthesize nanosprings so as to investigate their growth mechanisms [Gao, Ding, Mai, Hughes, Lao, and Wang (2005), Wang (2004), Amelinckx, Zhang, Bernaerts, Zhang, Ivanov, and Nagy (1994), McIlroy, Zhang, Kranov, and Norton

[1] National Chung Cheng University, Chia-Yi, Taiwan.

(2001), McIlroy, Alkhateeb, Zhang, Aston, Marcy, and Norton (2004), He, Fu, Zhang, Zhao, Zhang, Xia, and Cai (2007), Bell, Sun, Zhang, Dong, Nelson, and Grutzmacher (2006)]. It is observed that the cross-sectional shape of nanosprings varies from circle, ellipse to rectangle [McIlroy, Zhang, Kranov, Norton (2001), McIlroy, Alkhateeb, Zhang, Aston, Marcy, Norton (2004), Wang (2004)] possibly due to the differences in stress and strain during formation. Despite the initial successful growth of the helical or coiled structures, the consistent fabrication control of the nanosprings is still a subject of great research interest to many researchers.

There are several experimental attempts to characterize the physical and mechanical properties of these nanospring structures using scanning transmission microscopy (STM), atomic force microscopy (AFM), and transmission electron microscopy (TEM). Volodin, Ahlskog, Seynaeve, Van Haesendonck, Fonseca, and Nagy (2003) studied the elastic properties of coiled multiwalled nanotubes using AFM combined with a circular beam approximation and observed that the Young's modulus remains comparable to the hexagonal graphene sheets, which agree with the classical theory of elasticity. Chen, Zhang, Dikin, Ding, Ruoff, Pan, and Nakayama (2003) loaded a carbon nanocoil with two AFM tips and observed that the nanocoil behaves like an elastic spring in the low-strain regime with an elastic constant upturn in the high-strain regime. Singh, Liu, Ye, Picu, Lu, and Wang (2004) compressed the cobalt coated silicon nanospring by passing through a dc using a conductive AFM tip and found that the spring constant determined from the measurements was consistent with that obtained from a finite element analysis.

In addition to experimental characterization of the nanospring elastic properties, some researchers adopted continuum approaches to derive expressions for the nanospring stiffness [Da Fonseca, Malta, and Galvao (2006a)(2006b)]. However, it is still an unsettled question whether classical theory could apply to predict the behaviors of nanostructures and to what extent it can apply at the nanoscale. Molecular simulation method is a proper and frequently used tool to study the mechanical properties of nanostructures [Chen, Cheng, and Hsu (2007), Nair, Farkas, and Kriz (2008), Nishidate, and Nikishkov (2008)]. Chang and Yeh (2008) studied the elastic properties of circular cross-sectional nanospring using molecular statics method and found that some modifications need to be made to the classical equations in order to apply in the stiffness prediction of nanosprings.

In this research, we will focus on the atomistic study of elliptic cross-sectional nanospring. A series of systematic simulations will be performed to study the geometric size, cross-sectional shape and crystal orientation effect on the stiffness of the nanospring based on molecular statics calculation.

2 Molecular simulation

The suitable interatomic potentials and atomic model are essential to perform a proper molecular simulation. Without loss of generality, fcc copper is chosen for this study with lattice constant of 3.615 Å. The embedded-atom-method EAM potential developed by Foiles, Baskes, and Daw (1986) is chosen to describe atomic interactions. Among the various types of n-body potentials, the EAM potential is one of the most realistic and promising potentials, which provide a relevant description of the surface effect and defect properties of the transition metals with either a fcc or bcc structure. [Johnson (1988)(1989)] In the EAM potential, the total energy is composed of the electrostatic pairwise interaction energy between atoms and the embedding energy required to insert the atom into the local electron density field created by its near neighbors. Empirical functions in the EAM potential are fitted to experimentally measured bulk material properties, such as equilibrium lattice constants, sublimation energies, elastic constants, and vacancy formation energy.

Both normal and binormal nanosprings as shown in Fig. 1(a) and Fig. 2(a) are studied since they may lead to different technological application. The atomic model of nanosprings is constructed by firstly creating a large block of fcc single-crystalline copper atoms and keeping the atoms that are within the elliptic cross section, whose surface normal is perpendicular to the z axis, along the nanospring centerline as shown in Fig. 1(b) and Fig. 2(b). The semi-axes of the elliptic cross-sectional nanosprings are a and b, respectively. The cross section becomes circular while semiaxes a and b are equal. The spatial relation of the nanospring centerline can be described by

$$\vec{s} = R\cos\theta\hat{i} + R\sin\theta\hat{j} + \frac{\theta}{2\pi}P\hat{k}$$

where R and P are the radius and pitch of the nanospring helix, respectively. The vertical displacement will shift a pitch when θ rotates an angle of 2π and, thus, the spring rising angle α is defined as $\tan\alpha = P/2\pi R$. Only one full pitch length of the nanospring is constructed in the atomic model. The periodic boundary condition (PBC) is applied in the z direction to simulate an infinitely long nanospring. Uniaxial strain deformation along z direction is loaded on nanosprings to extract their elastic properties.

In this research, various sizes of nanosprings are built to investigate the dependence of the nanospring radius, pitch, and wire semi-axis length (i.e. a- and b-axis). The radii R of the nanosprings are in the range of 6-9 nm, the wire semi-axes are 5-8 nm, and the pitches are 20-35 nm, as listed in Tab. 1. The numbers of atoms in the simulation model are 55036-100294, respectively. Meanwhile, three different arrangements of nanospring crystallographic orientations are considered as shown

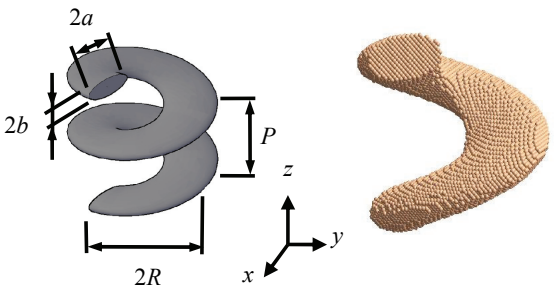

Figure 1: The schematic presentation of the normal nanospring. (a) The geometry and (b) the atomic model.

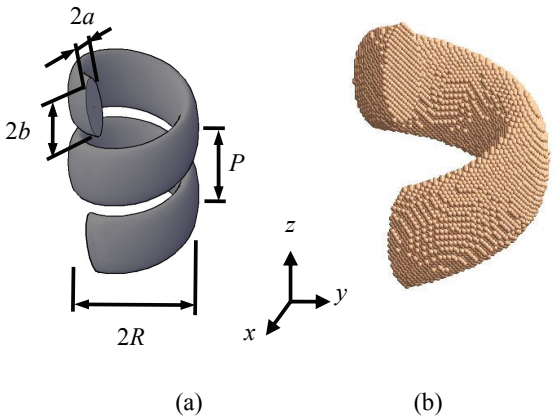

Figure 2: The schematic presentation of the binormal nanospring. (a) The geometry and (b) the atomic model.

in Fig. 3 to illustrate the crystal orientation dependence.

Molecular statics simulations are implemented using the conjugate gradient method to carry out the energy minimization process so that the equilibrium atomic structure could be obtained. The considered energy includes the potential energy of interatomic interactions and potential energy due to external loading. Because the initial atomic positions of the nanospring might not be in their equilibrium condition, the model is fully relaxed by adjusting the periodic length in the z direction to eliminate the nonzero initial stresses. Since there is no constraint applied in the

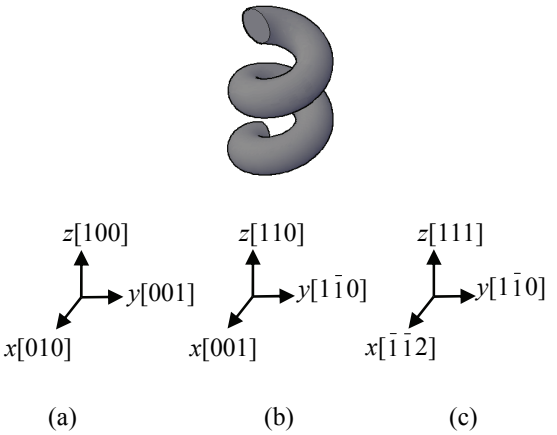

Figure 3: The schematic presentation of the nanosprings with different crystallographic orientations: (a) [100], (b) [110], and (c) [111] nanosprings.

x and y directions, the stresses in these two directions will automatically approach zero. After reaching the equilibrium, the system energy of the nanospring model will be the lowest, which is also set as the zero-energy point.

Then, a small uniform tensile or compressive displacement along z direction is applied step by step on the equilibrated atomic model. The application of loading displacement is accomplished by uniformly expanding or contracting the periodic length in the direction of deformation. After each step of the loading process, the atoms are allowed to equilibrate within the changed dimensions and current minimum energy positions are computed. Following each loading step, the system energies of the nanospring are recorded as in Fig. 4. It is found that the system energies increase as the tensile or compressive loadings increase and the energy-loading curve is a parabola. Using the parabolic equation, $U = \frac{1}{2}Kd^2$, to curve fit the energy-loading relation, the spring constant of the nanospring, K, could be calculated. The spring constant is determined from the parabolic curve best fit to the displacement-energy curve.

3 Results

Molecular statics approach is utilized to simulate the uniaxial tensile and compressive test of elliptic cross-sectional nanosprings. The size and crystal orientation effects on elastic behaviors are studied and the elastic constants calculated from the energy-loading relation are systematically compared. The atomic structures of nanosprings at the equilibrium are examined and it is found that the initial shapes

Table 1: The geometric parameters of the normal and binormal nanospring models

Model	R (nm)	$2a$ (nm)	$2b$ (nm)	P (nm)	α ($^\circ$)
N	6	8	5	20	27.9
NR1	7	8	5	20	24.5
NR2	8	8	5	20	21.7
NR3	9	8	5	20	19.5
Nt1	6	5	5	20	27.9
Nt2	6	6	5	20	27.9
Nt3	6	7	5	20	27.9
NP1	6	8	5	25	33.6
NP2	6	8	5	30	38.5
NP3	6	8	5	35	42.9
B	6	5	8	20	27.9
BR1	7	5	8	20	24.5
BR2	8	5	8	20	21.7
BR3	9	5	8	20	19.5
Bt1	6	5	5	20	27.9
Bt2	6	5	6	20	27.9
Bt3	6	5	7	20	27.9
BP1	6	5	8	25	33.6
BP2	6	5	8	30	38.5
BP3	6	5	8	35	42.9

are preserved as plotted in Fig. 5(a). Moreover, it is noticed that the equilibrated nanosprings still maintain the crystalline fcc structure from the radial distribution function (RDF) as depicted in Fig. 5(b).

As illustrated in Fig. 6(a), the spring constants of both normal and binormal nanosprings increase as the wire semi-axis length become larger irrespective to the crystal orientations. It is noted that the stiffness increases more drastically as the semi-axis a increases for normal nanosprings (N, Nt series) than the semi-axis b for binormal ones (B, Bt series). As the radii and pitches of the nanosprings increase, the stiffness of the nanosprings becomes smaller as shown in Fig. 6(b) and 6(c). It is observed that [100] nanosprings are stiffer than both [110] and [111] ones for both normal and binormal nanosprings. Moreover, the normal nanosprings (N, Nt, NR, NP series) always behave stiffer than the binormal ones (B, Bt, BR, BP series) for the same radius, pitch and cross-sectional geometry in the comparison.

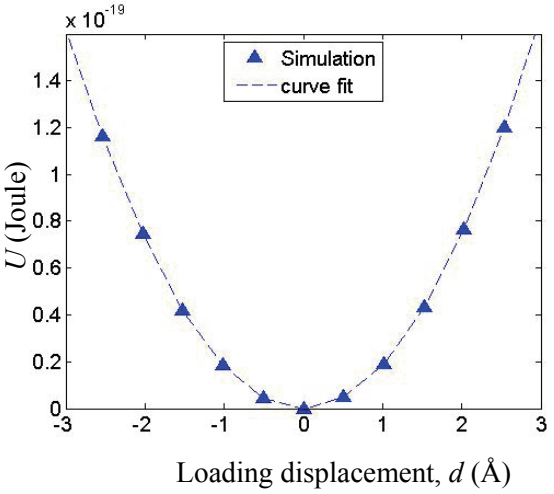

Figure 4: The relationship between the nanospring system energy and loading displacement for nanospring model.

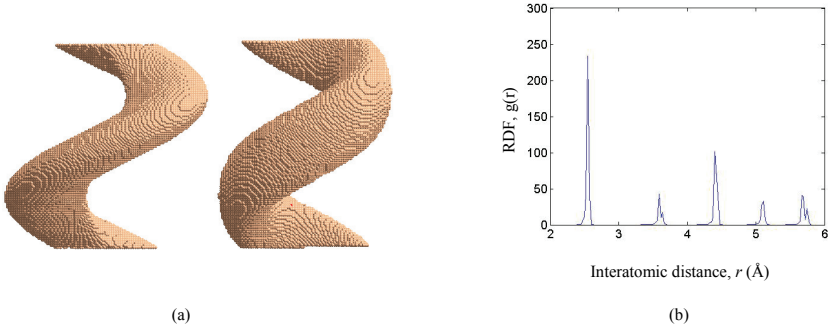

Figure 5: [100] nanospring at the equilibrium: (a) the atomic structure for normal (model N) and binormal (model B) nanosprings and (b) RDF.

4 Discussion

In this research, the geometric size, cross-sectional shape (normal and binormal) and crystal orientation effects on the elastic behaviors of nanosprings are systematically studied using molecular statics method. Without consideration of the velocity term, the computation time for molecular statics method is relatively shorter as compared to those for other molecular methods. However, molecular statics simulation is limited to 0 K temperature also due to its lack of velocity term and the

loading process is considered quasi-static unlike the high loading rate in molecular dynamics simulation. As discussed by Chang and Chen (2007), molecular statics method could adequately calculate the elastic properties of nanomaterials as the molecular dynamics simulation at low temperature and the trend in size dependence of elastic behavior would not be altered by temperature.

The dependences of nanospring stiffness on the geometric parameters (radius, wire semi-axis length and pitch) are further analyzed based on the derived expression by Da Fonseca, Malta, and Galvao (2006a,b) using the continuum Kirchhoff rod model

$$K = \frac{Ea^3 b \cos\alpha}{8NR^3}$$

where E is Young's modulus of the nanospring material and N is the number of turns. Indeed, a linear relationship is observed between the elastic constants and the simulated wire semi-axis length (a^3b), the inverse of the third order of radii as well as the cosine of the rising angle irrespective to the crystal orientations as shown in Fig. 7(a), (b) and (c). It is noticed that [100] nanosprings are always stiffer than both [110] and [111] ones for the same geometric size no matter normal or binormal nanosprings.

Besides, it is found that the simulation results collapse into individual master lines for respective crystal orientations and cross-sectional shape (normal and binormal) as illustrated in Fig. 8, which suggests that the classic equation predicts well the relationship between the stiffness and the nanospring radius and wire semi-axis length combining with the rising angle as $K \propto \frac{a^3 b}{R^3}\cos\alpha$ for elliptic cross-sectional nanosprings. However, the slopes of individual master curve are different, which indicates that the Young's modulus is not the same for different crystal orientation. This can be realized by the amorphous material assumption made by Da Fonseca, Malta, and Galvao (2006b) in their derivation while the single crystalline copper nanosprings investigated in our research are not made of isotropic materials.

5 Concluding remarks

In this work, molecular statics method with EAM potential is employed to study single-crystalline copper nanosprings with elliptical cross sections. Several geometric sizes, cross-sectional shape (normal and binormal) and crystal orientations of nanosprings are systematically simulated in order to investigate the elastic constant dependence. It is shown consistently that the elastic constants of nanosprings are observed to increase as the semi-axis length increases, while the radius and pitch decrease irrespective to the crystal orientation of the nanospring. It is shown that two nanosprings of the same cross-sectional geometry, radius and pitch but

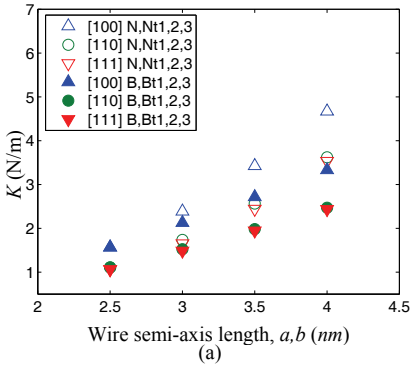

(a)

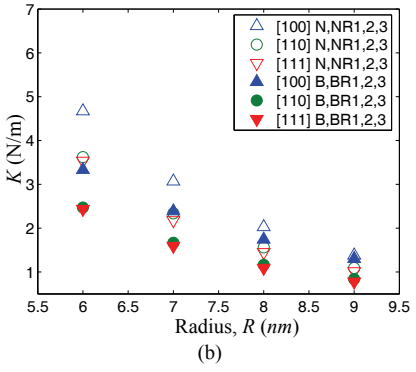

(b)

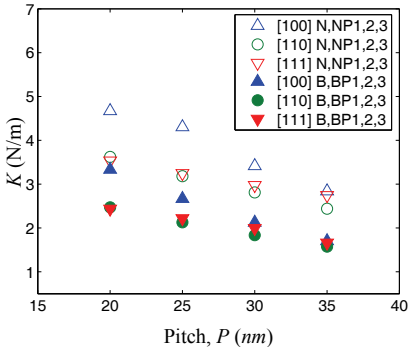

(c)

Figure 6: The size dependences of elastic constants for normal and binormal nanosprings with different crystal orientations. (a) Wire semi-axis length, (b) radius, and (c) pitch.

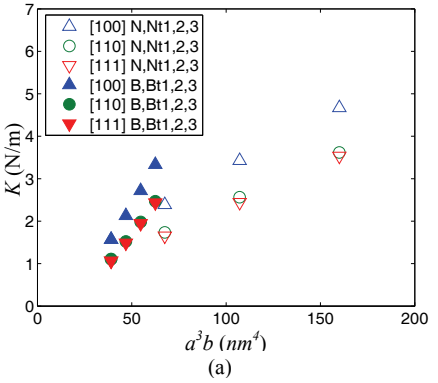

(a)

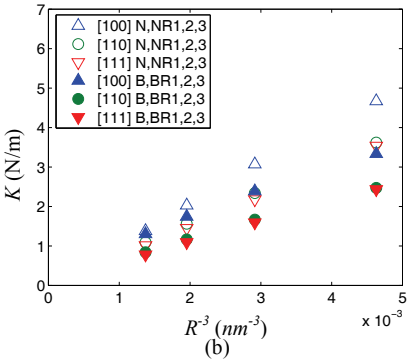

(b)

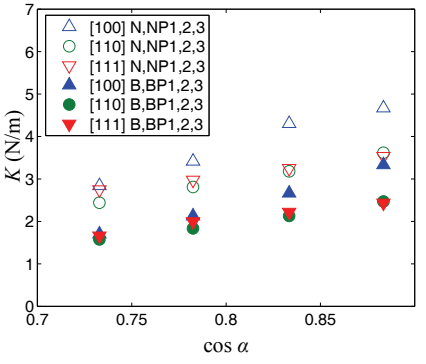

(c)

Figure 7: The size dependences of elastic constants for different crystallographic oriented nanosprings: (a) wire semi-axis length, (b) radius, and (c) rising angle.

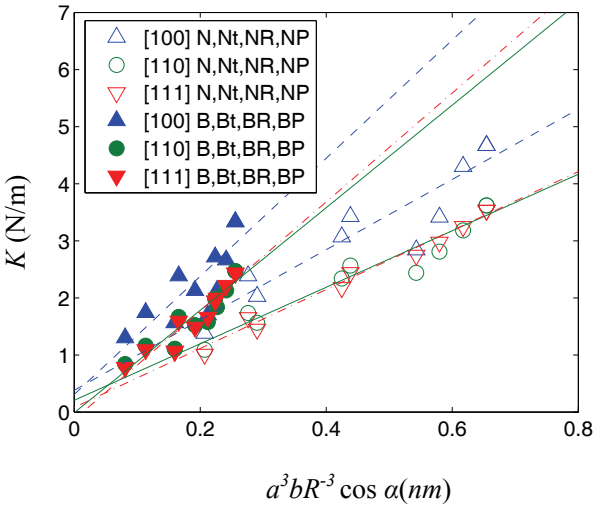

Figure 8: The size dependences of elastic constants for different crystallographic orientated nanosprings.

differing by the fact that one is a normal structure and the other is binormal, have different stiffness. In our study, the normal nanospring is always stiffer than the binormal one. Furthermore, it is concluded that the classical equations derived based on continuum theory could predict the elastic behavior of elliptic cross-sectional nanospring quite well.

Acknowledgement: This research work is supported by National Science Council of Taiwan under the grant NSC-97-2221-E-194-015.

References

Amelinckx, S.; Zhang, X. B.; Bernaerts, D.; Zhang, X. F.; Ivanov, V.; Nagy, J. B. (1994): A formation mechanism for catalytically grown helix-shaped graphite nanotubes. *Science*, vol. 265, pp. 635-639.

Bell, D. J.; Sun, Y.; Zhang, L.; Dong, L. X.; Nelson, B. J.; Grutzmacher, D. (2006): Three-dimensional nanosprings for electromechanical sensors. *Sensors and Actuators A*, vol. 130-131, pp. 54-61.

Chang, I.-L.; Chen, Y.-C. (2007): Is molecular statics method suitable for the study of nanomaterials? The study case of nanowires. *Nanotechnology*, vol. 18, pp. 315701.

Chang, I-L.; Yeh, M.-S. (2008): An atomistic study of nanosprings. *J Applied Physics*, vol. 104, pp. 024305.

Chen, W. H.; Cheng, H. C.; Hsu, Y. C. (2007): Mechanical properties of carbon nanotubes using molecular dynamics simulations with the inlayer van der waals Interactions. *CMES: Computer Modeling in Engineering & Sciences,* vol. 20, pp. 123-145.

Chen, X.; Zhang, S.; Dikin, D. A.; Ding, W.; Ruoff, R. S.; Pan, L.; Nakayama, Y. (2003): Mechanics of a carbon nanocoil. *Nano Letters*, vol. 3, pp. 1299-1304.

Da Fonseca, A. F.; Malta, C. P.; Galvao, D. S. (2006a): Elastic properties of nanowires. *J Applied Physics*, vol. 99, pp. 094310.

Da Fonseca, A. F.; Malta, C. P.; Galvao, D. S. (2006b): Mechanical properties of amorphous nanosprings. *Nanotechnology*, vol. 17, pp. 5620-5626.

Foiles, S. M.; Baskes, M. I.; Daw, M. S. (1986): Embedded-atom-method functions for the fcc metals Cu, Ag, Au, Ni, Pd, Pt, and their alloy. *Physical Review B*, vol. 33, pp. 7983-7991.

Gao, P. X.; Ding, Y.; Mai, W.; Hughes, W. L.; Lao, C.; Wang, Z. L. (2005): Conversion of zinc oxide Nnanobelts into superlattice-structured nanohelices. *Science*, vol. 309, pp. 1700-1704.

He, Y.; Fu, J.; Zhang, Y.; Zhao, Y.; Zhang, L.; Xia, A.; Cai, J. (2007): Multilayered Si/Ni nanosprings and their magnetic properties. *Small*, vol. 3, pp. 153-160.

Johnson, R. A. (1988): Analytic nearest-neighbor model for fcc metals. *Physical Review B*, vol. 37, pp. 3924-3931.

Johnson, R. A. (1989): Alloy models with the embedded-atom method. *Physical Review B*, vol. 39, pp. 12554-12559.

McIlroy, D. N.; Zhang, D.; Kranov, Y.; Norton, M. G. (2001): Nanosprings. *Applied Physics Letters*, vol. 79, pp. 1540-1542.

McIlroy, D. N.; Alkhateeb, A.; Zhang, D.; Aston, D. E.; Marcy, A. C.; Norton, M. G. (2004): Nanospring formation-unexpected catalyst mediated growth. *J Physics: Condensed Matter*, vol. 16, pp. R415-R440

Nair, A. K.; Farkas, D.; Kriz, R. D. (2008): Molecular dynamics study of size effects and deformation of thin films due to nanoindentation. *CMES: Computer Modeling in Engineering & Sciences,* vol. 24, pp. 239-248.

Nishidate, Y.; Nikishkov, G. P. (2008): Atomic-scale modeling of self-positioning nanostructures. *CMES: Computer Modeling in Engineering & Sciences,* vol. 26, pp. 91-106.

Singh, J. P.; Liu, D.-L.; Ye, D.-X.; Picu, R. C.; Lu, T.-M.; Wang, G.-C. (2004):

Metal-coated Si springs: Nanoelectromechanical actuators. *Applied Physics Letters,* vol. 84, pp. 3657-3659.

Volodin, A.; Ahlskog, M.; Seynaeve, E.; Van Haesendonck, C.; Fonseca, A.; Nagy, J. B. (2003): Imaging the elastic properties of coiled carbon nanotubes with atomic force microscopy. *Physical Review Letters*, vol. 84, pp. 3342-3345.

Wang, Z. L. (2004): Nanostructures of zinc oxide. *Materials Today*, vol. 7, pp. 26-33.